Radiol Phys Technol (2016) 9:139–153
DOI 10.1007/s12194-016-0361-6

Dynamic chest radiography: flat-panel detector (FPD) based functional X-ray imaging

Rie Tanaka[1]

Received: 13 May 2016 / Revised: 16 May 2016 / Accepted: 18 May 2016 / Published online: 13 June 2016

Abstract Dynamic chest radiography is a flat-panel detector (FPD)-based functional X-ray imaging, which is performed as an additional examination in chest radiography. The large field of view (FOV) of FPDs permits real-time observation of the entire lungs and simultaneous right-and-left evaluation of diaphragm kinetics. Most importantly, dynamic chest radiography provides pulmonary ventilation and circulation findings as slight changes in pixel value even without the use of contrast media; the interpretation is challenging and crucial for a better understanding of pulmonary function. The basic concept was proposed in the 1980s; however, it was not realized until the 2010s because of technical limitations. Dynamic FPDs and advanced digital image processing played a key role for clinical application of dynamic chest radiography. Pulmonary ventilation and circulation can be quantified and visualized for the diagnosis of pulmonary diseases. Dynamic chest radiography can be deployed as a simple and rapid means of functional imaging in both routine and emergency medicine. Here, we focus on the evaluation of pulmonary ventilation and circulation. This review article describes the basic mechanism of imaging findings according to pulmonary/circulation physiology, followed by imaging procedures, analysis method, and diagnostic performance of dynamic chest radiography.

✉ Rie Tanaka
rie44@mhs.mp.kanazawa-u.ac.jp

[1] Department of Radiological Technology, School of Health Sciences, College of Medical, Pharmaceutical and Health Sciences, Kanazawa University, 5-11-80 Kodatsuno, Kanazawa 920-0942, Japan

Keywords Chest radiography · Functional imaging · Flat-panel detector (FPD) · Ventilation · Circulation · Dynamic image analysis

1 Background

Over the last 50 years or so, many investigators have contributed to the development of a pulmonary functional imaging method based on X-ray technique. Their approaches progressed from X-ray densitometry to image intensifier (II) TV digital imaging, and now dynamic flat-panel detector (FPD) imaging.

From the beginning, there has been concern about analysis of the changing lung density during respiration. Kourilsky and his associates [1] first described a fluoroscopic technique with special photoelectric cells for lung density analysis during respiration. They achieved the detection of abnormalities as small variations in video signals. Since then, variations of their procedure have been used by others, confirming its usefulness [2–4]. Modifications of this technique known as fluorodensitometry and video densitometry were proposed by George et al. [5, 6] and Siverman et al. [7–9], respectively. They differentiated ventilation abnormalities from normal regions. During the same period, other groups were dedicated to the development of image-oriented technology. Rogers et al. [10] and Toffolo et al. [11] evaluated the distribution of intravenous radioactive agents by scanning one whole lung, using collimators with 1–2 cm diameter.

In the 1980s, II-TV systems were commonly used in clinical practice. Researchers attempted to visualize pulmonary ventilation and circulation based on the translucency variations on digital fluoroscopic images, for which they used the subtraction technique. Leung et al. [12, 13]

investigated regional pulmonary ventilation with a 57 cm II-TV system and nonradioactive Xenon. Regional pulmonary and myocardial perfusion with digital subtraction angiography (DSA) was proposed in this period [14–16]. The digital subtraction technique without any injection was also proposed and proven to be useful for studying ventilation and/or perfusion on digital fluoroscopic images [17–19]; this was the precursor of dynamic chest radiography.

Although there have been many reports demonstrating the feasibility of pulmonary densitometry and digital fluoroscopic approaches, these techniques have not achieved widespread use due to technical limitations, such as the need for special instrumentation, poor image quality, and a small field of view (FOV).

Dynamic chest radiography based on a dynamic FPD combined with computer analysis has overcome the difficulties encountered in the above mentioned studies. Dynamic FPDs were developed in the 2000s and are now widely used in X-ray fluoroscopic examinations. With dynamic FPDs, both lungs can be observed simultaneously on dynamic images during respiration with a large FOV. There is no image distortion, and high image quality can be achieved at low dose levels due to improved sensitivity of X-ray detectors [20, 21].

Dynamic chest radiographs contain a wealth of functional information, such as diaphragm movement, cardiac motion, pulmonary ventilation, and circulation. Most importantly, pulmonary ventilation and circulation are reflected as slight changes in pixel value on dynamic chest radiographs. However, their interpretation is challenging for radiologists; therefore, computerized methods have been developed for the evaluation of pulmonary ventilation [22–25] and circulation [26–29] on dynamic chest radiographs. With image subtraction and color-mapping techniques, ventilatory and perfusion impairments were detected as reduced changes in pixel value without the use of contrast media (described later in detail).

The first clinical report of this technique was published by the author's group [22]. We demonstrated that in a patient with emphysema, trapped air was indicated as reduced changes in pixel value despite diaphragm motion in a dynamic way. In experimental studies focusing on pulmonary perfusion, we also succeeded in visualizing circulation-caused changes in pixel value as sequential map of blood distribution, showing a normal pattern, which diffuses from around the pulmonary arteries to the peripheral area [26, 28]. In the process of functional analysis, many related technologies have been developed for evaluating diaphragm motion [30, 31], measuring the velocity field in the lungs [31], and determining the respiratory/cardiac phase [30–32].

The diagnostic performance improved as technology advanced, and finally, a functional X-ray imaging method, called "dynamic chest radiography", was realized. It is expected to be a low dose and cost-effective functional imaging method for evaluation of pulmonary function.

2 Physiology: what is reflected on dynamic chest radiographs?

The most common and simple form of functional imaging is inspiratory/expiratory chest radiography. In general, additional imaging at the expiration level is performed for assessment of diaphragm movement and respiration-induced changes in X-ray translucency in the lungs, in addition to conventional imaging at the inspiratory level. Dynamic chest radiography also focuses on the lung density changes due to respiration or circulation. It is essential to understand their mechanism in terms of pulmonary and circulation physiology for utilizing dynamic chest radiography as a powerful and pertinent radiologic tool.

2.1 Pulmonary ventilation

The condition of the lungs is evaluated on the basis of X-ray translucency in the lung area in conventional chest radiographs. An increase in X-ray translucency indicates localized air space that may represent anomalies like a lung cyst, emphysema, bulla, and pneumothorax. In contrast, a decrease in X-ray translucency indicates decreased pulmonary air or enhanced tissues, suggestive of conditions like pulmonary inflammation, fibrosis, edema, or sclerosis [33]. In dynamic chest radiographs, pulmonary function can be assessed based on the temporal changes in X-ray translucency due to respiration or cardiac pumping. The respiration-induced changes depend on relative increases and decreases in the air and lung vessel volume per unit volume [34, 35].

Figure 1 depicts the measured pixel value and electrocardiogram (ECG) findings in a normal control subject. Low pixel values were related to dark areas in the images, and these in turn, were related to high X-ray translucency in this review article. The pixel value decreases (X-ray translucency↑) according to an increase in air volume in the lung during the inspiratory phase; in contrast, the pixel value increases (X-ray translucency↓) according to a decrease in air volume in the lung during the expiratory phase. The slight change in synchrony with ECG findings is the result of changes caused by cardiac pumping and pulmonary blood circulation. The impact of cardiac motion is identified to be less than 10 % on the respiration-induced changes [36]. Thus, it is possible to evaluate the relative pulmonary ventilation quantitatively from respiration-

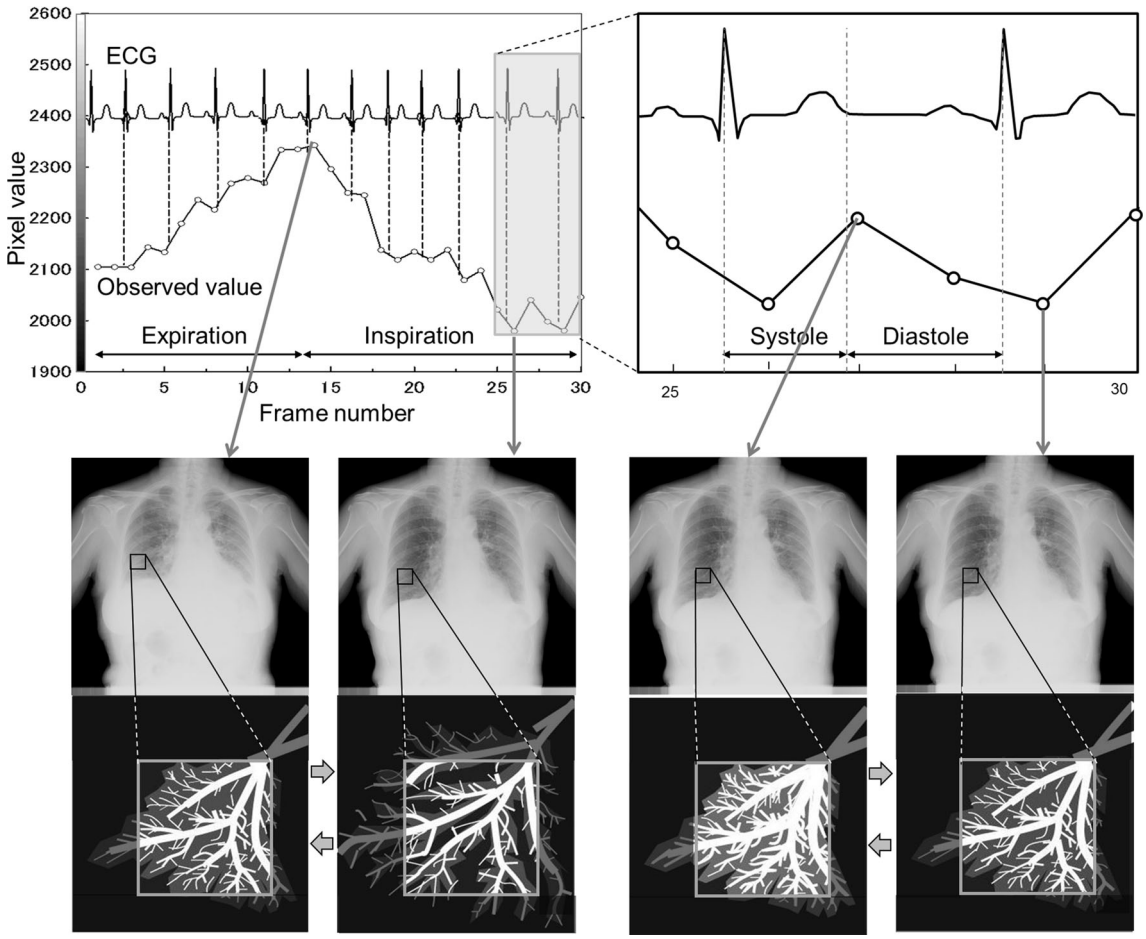

Fig. 1 Mechanism of dynamic changes in X-ray translucency (= pixel value). Respiration-induced changes in pixel value are caused by changes in air and lung vessel volume per unit volume, whereas circulation-induced ones are caused by changes in blood volume per unit volume

induced changes in pixel value on dynamic chest radiographs.

For example, chronic obstructive pulmonary disease (COPD) patients take time to expire, and they also ventilate insufficiently due to trapped air. Therefore, it is possible to detect abnormalities such as delayed and decreased changes in pixel values. Preliminary studies showed that a simulated ventilatory defect more than 10 mm in diameter could be detected as decreased changes in pixel value. In addition, respiratory changes in pixel value had a close relationship with displacement of the diaphragm, and the changes in the right and left lungs were almost the same (R:L = 1:1) [37]. However, the following points should be noted: the present method does not directly measure the gas exchanges in the lung alveoli; rather, it provides relative functional information related to pulmonary ventilation.

2.2 Regional differences in ventilation

It is well known that there are regional differences in ventilation in respiratory physiology [34, 35]. Ventilation per unit volume is greatest near the bottom of the lung and becomes progressively smaller toward the top, with a symmetrical right-and-left distribution. Therefore, in clinical situations, ventilatory impairment can be detected based on a deviation from the normal pattern of the ventilation distribution. In the same way, regional differences in ventilation can be detected as regional differences in respiratory changes in pixel value, which are greatest near the bottom of the lung and become significantly smaller toward the top ($P < 0.01$) [37]. Therefore, ventilatory impairment can be detected by comparison of respiration-induced changes in pixel value in the left and right lungs in the craniocaudally same level [25]. These facts show that dynamic chest radiography has the capability of measuring "regional differences in ventilation" based on the respiration-induced pixel value.

2.3 Airway closure

At the end of expiration, the lower airway closes earlier than the upper airway due to the differences in air pressure

of the thoracic cavity, i.e., airway closure, and the ventilation in the upper area becomes greater than that in the lower area [35]. The lung volume when airway closure occurs is defined as the "closing volume," which is a very effective index for diagnosing pulmonary diseases. For example, in subjects with COPD and restrictive pulmonary disease, airway closure appears in the early expiratory phase, and as a result the closing volume becomes large. Therefore, abnormalities can be detected by evaluation of the timing of "airway closure". In the case of dynamic chest radiography, airway closure is confirmed as moving up of regions with the greatest inter-frame differences in pixel value during expiration [37]. That is, dynamic chest radiography has the capability of determining the "closing volume" based on the regional and temporal measurement of the respiration-induced changes in pixel value.

2.4 Pulmonary blood flow

Circulation dynamics is reflected on chest radiographs, and abnormalities appear as shape changes or shifts in the distribution of pulmonary vessels [35, 38, 39]. These are effective indices for diagnosing specific cardiac diseases and determination of an appropriate examination procedure: redistribution or cephalization of pulmonary blood flow, indicating the presence of pulmonary venous hypertension [40]; a centralized pulmonary blood flow pattern, indicating pulmonary arterial hypertension [41]; or widening of the vascular pedicle, indicating an increase in the circulating blood volume [42]. Circulation dynamics is also reflected on fluoroscopic images as changes in X-ray translucency [8, 9, 26–28] (Fig. 1), which provide functional information. This is because the lungs contain a constant volume of about 500 mL of blood, with 75 mL distributed variably across the vasculature due to cardiac pumping [36].

In dynamic FPD imaging; the pixel values change linearly with the blood volume in the lungs, and a perfusion defect more than 10 mm in diameter can be detected as decreased changes in pixel values [26]. There is a concern about dilation and contraction of vessels; however, it would not be considered to affect the measurement of pixel values in projected images because the rate of change is reported to be approximately ±10 % [25].

Figure 2 shows changes in pixel value measured in regions of interest (ROIs) on dynamic chest radiographs under breath-holding in a normal subject. There is a strong correlation between the cardiac cycle and changes in pixel value, which are measured in the ventricles, atria, aortic arch, and pulmonary arteries [25] (Fig. 2a, b). The changes in pixel values measured in each ROI can be explained by normal circulation dynamics, as indicated below: (1) at the end of the diastolic phase, the ventricles are at the maximum volume, as shown by large pixel values in the ventricles. (2) In the early ventricular systolic phase, from closure of the atrioventricular (AV) valves to opening of the aortic valve, the ventricular volume remains constant, shown as the absence of a significant change in pixel values during this period. (3) After opening of the aortic valve, blood is pumped from the ventricles into the aortic arch and pulmonary arteries. This is shown as decrease in pixel values in the ventricles and an increase in pixel values in the aortic arch and pulmonary arteries. (4) In the late ventricular systolic phase, increase in aortic blood flow is shown as a continuous increase in pixel values. (5) In the early ventricular diastolic phase, from closure of the aortic valve to opening of the AV valves, the ventricular volume remains constant. (6) Blood rapidly moves from the atria to the ventricles in response to opening of the AV valves; this is why the pixel values in the ventricles increase, while those in the atria and pulmonary veins decrease.

Figure 2c shows the average rate of change in pixel value for seven normal subjects. The results measured in each ROI decrease in the following order: left ventricle > left atrium > aortic arch > right atrium > right ventricle > left pulmonary artery. These findings indicate that the pulmonary blood circulation is reflected on dynamic chest radiographs, and that the quantitative analysis of changes in pixel value has potential for evaluation of the local blood circulation.

3 Imaging procedures

Sequential chest radiographs during forced respiration are obtained with use of a dynamic FPD system and X-ray generator capable of pulsed irradiation. To be a reliable diagnostic tool, the system must have a high homogeneity and uniformity in X-ray pulses [43]. Except for breathing manner, imaging is performed in the same way as the conventional chest examination, i.e., the standing position and the PA (posteroanterior) direction. For an accurate evaluation of cardiopulmonary function, it is crucial to include one respiratory cycle within a limited amount of time with good reproducibility. Therefore, it is recommended to use an automatic voice system and conduct pretraining for patients. The total patient dose is adjustable by changes in the imaging time, imaging rate, and source to image distance (SID), and can be less than the dose limit for two projections (PA + LA) recommended by the International Atomic Energy Agency (IAEA) (1.9 mGy) [44].

Cardiopulmonary function is evaluated separately in each respiratory phase, i.e., inspiratory, expiratory, and breath-holding phase. The imaging rate should be greater than 7.5 frames per second (fps) to permit an accurate

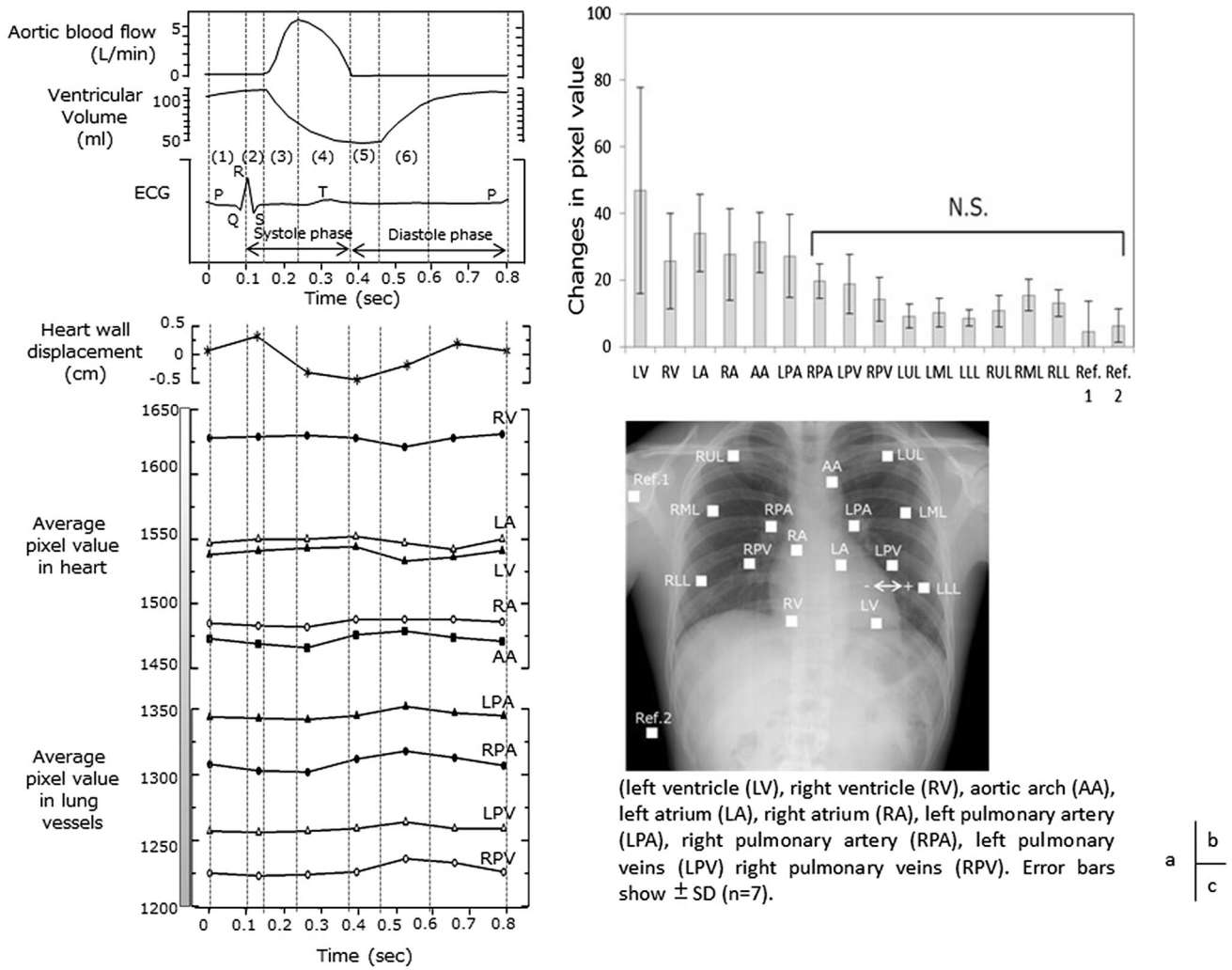

(left ventricle (LV), right ventricle (RV), aortic arch (AA), left atrium (LA), right atrium (RA), left pulmonary artery (LPA), right pulmonary artery (RPA), left pulmonary veins (LPV) right pulmonary veins (RPV). Error bars show ± SD (n=7).

Fig. 2 (a) Relationship between cardiac cycle and changes in pixel values, (b) the variations during a whole cycle, and (c) measurement locations. Small squares show ROIs for measuring average pixel value, and the horizontal line shows a profile for measuring left ventricle motion. (SD: standard deviation, N.S.: not significant)

evaluation of cardiac function [26]. If the focus is on the evaluation of respiratory function, a lower imaging rate than 7.5 fps is acceptable by taking into account the patient dose. However, an imaging time of more than 10 s is required to induce the maximum voluntary respiration. Figure 3 shows an example of the imaging protocol. In the case that the exposures are taken at 120 kV, 50 mA, 2.5 ms, 15 fps, and 2.0 m of SID, the entrance surface dose to the detector is approximately 1.9 mGy in 14 s.

4 Dynamic image analysis

Dynamic chest radiographs are sequential chest radiographs obtained in an extremely short time interval. Thus, we can utilize some of the previously developed image processing techniques for conventional chest radiographs, such as recognition of the lung area [45, 46], texture analysis [47–51], measurement of heart size [52], and image registration [53, 54], as well as recursive filter [55] and motion tracking [56–58] for digital fluoroscopy or DSA. To extract functional information from dynamic chest radiographs, we need to develop dynamic-oriented analysis methods, while effectively utilizing the techniques described above. The computerized scheme for dynamic chest radiographs includes three basic components: determination of imaging phase, quantification, and visualization of functional information, as shown in Fig. 4.

4.1 Image pre-processing

Dynamic chest radiographs consist of images during the inspiration, expiration, and breath-holding phases, which

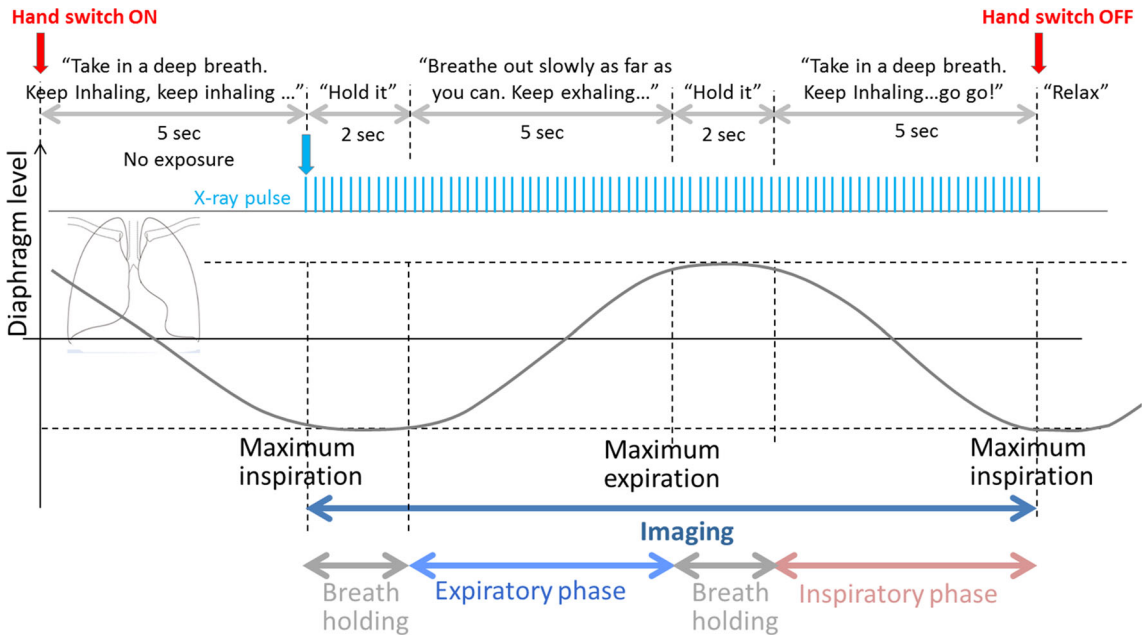

Fig. 3 An example of imaging protocol for dynamic chest radiography

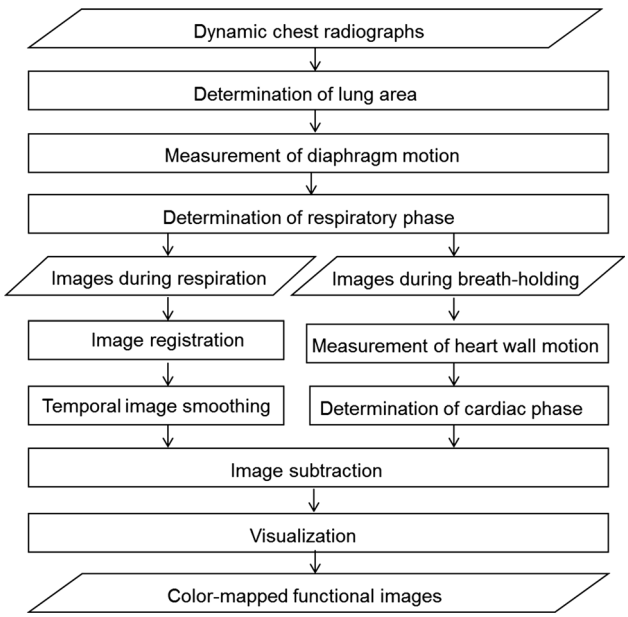

Fig. 4 Overall scheme of image analysis for dynamic chest radiographs

are classified into any of the cardiac phases, systole or diastole. It is essential to specify the respiratory and cardiac phases of each image because dynamic images contain different kinetic information in each respiratory and cardiac phase. For selecting proper image processing, the respiratory and cardiac phases should be determined prior to dynamic image analysis.

4.1.1 Determination of respiratory phase

The lung area is determined by edge detection using the first derivative technique and an iterative contour-smoothing algorithm [45, 46]. The upper most points of the lung and diaphragm are determined in the first frame, and then traced by the template-matching technique after the second frame [22, 30, 31]. The respiratory phase is determined based on the distance from the lung apex to diaphragm. The frames for the maximum and minimum distance are determined as the maximum inspiratory and expiratory frames, respectively [32]. In this process, the excursion of the diaphragm is also calculated by subtracting the distance at the maximum inspiratory level from that at the expiratory level. Diaphragm kinetics provides effective functional information for the diagnosis of pulmonary diseases. Abnormalities are detected by comparison with normal excursion or side-by-side comparison in each individual.

4.1.2 Determination of cardiac phase

The cardiac phase is estimated on the basis of moving directions of the left ventricular wall, which can be determined by the motion tracking technique. In this approach, cardiac function can be assessed based on the motion rhythm and displacement of the left ventricle wall. The cardiac phase is also stably determined based on the averaged pixel values measured in a ROI over the edge of the left ventricular wall [28]. In that case, decrease in pixel values (a low proportion of the cardiac area) is determined

as the systolic phase and increase in pixel values (a high proportion of cardiac area) as the diastolic phase.

4.2 Quantification and visualization

Image subtraction is a powerful tool for identifying slight changes in pixel value, even though it is difficult to evaluate the changes by observing images. There are two main approaches to the quantification and visualization of pulmonary ventilation and circulation: (1) inter-frame subtraction, and (2) image subtraction with/among specific images (e.g., an averaged image, MIP/MinIP, an image in the maximum inspiration or expiration, an image in the systolic or diastolic phase, etc.). The former provides functional information relevant to "change rate" or "flow velocity", whereas the latter provides functional information relevant to "distribution".

MIP maximum intensity projection
MinIP minimum intensity projection

4.2.1 Pulmonary ventilation

Pulmonary ventilation is assessed in images during respiration. It is highly likely that the same point on sequential images does not represent the same anatomic point. Thus, a non-rigid image registration is required to match the corresponding points to each other. The image-warping technique developed for digital image subtraction of temporally sequential chest images can be utilized for this purpose [53]. The displacement of lung structures at the imaging rate of more than 7.5 fps is quite small, 0–3 pixels per frame. Therefore, a spatial smoothing may be used as an alternative for inter-frame registration. The spatial smoothing technique is effective in reducing respiratory artifacts caused by slight mis-registration of lung structures. Smoothing of pixel values is also performed in the time axis direction to reject noise due to circulation artifacts [22]. After the image registration and noise reduction, two kinds of image subtraction described below are performed.

Inter-frame differences in pixel value during respiration create velocity maps of respiration-caused changes in pixel value, i.e., information related to the change rate or velocity of the air flow. Figure 5 shows the overall scheme of the computer algorithm for visualizing respiration-caused changes. Inter-frame differences are calculated throughout all images during respiration, and are then superimposed on the original images in the form of a color display using a color table in which higher X-ray translucency (increased air) is shown in warm colors, and negative changes, i.e., lower X-ray translucency (decreased air) are shown in cool colors. As shown in Fig. 5, we can visually evaluate the regional changes in pixel value on the resulting maps, showing a normal pattern determined in pulmonary physiology [34, 35].

Image subtraction between images at the maximum inspiration and expiration creates another functional image, showing a distribution map of respiration-caused changes in pixel value, i.e., information related to the ventilation distribution. We can also evaluate the pulmonary function using difference maps created from image subtraction with any kind of specific image (e.g., an averaged image during one breathing cycle, an image in expiratory phases) as a base image. A base image varies depending on the diagnostic purpose. In any approach, these functional images are also created by superimpose of the difference values on dynamic chest radiographs in the form of a color display. The relative inspired volume compared to that at the maximum expiratory level may be assessed in a distribution map, while the relative increase and decrease in ventilation compared to the base image in difference maps, respectively.

4.2.2 Pulmonary circulation

Pulmonary circulation is assessed in images during breath-holding, which do not contain respiration-induced changes in pixel value. Spatial smoothing is used for reducing artifacts caused by pulsating lung structures. The pulmonary circulation may be analyzed in images during respiration. In that case, pre-processing is required so that respiratory changes in pixel value are rejected. A correction method developed for videodensitometry can be utilized for this purpose [9]. Signals measured over the edge of the heart are used as reference and correlated with those measured in various ROIs to produce signals with low noise to reduce respiratory artifacts. These correlations are performed as a function of time delay between the reference signal and the noisy densitometry signal.

Figure 6 shows the overall scheme of the computer algorithm for visualizing the pulmonary circulation. Inter-frame differences in pixel value during breath-holding create velocity maps of circulation-caused changes in pixel value, i.e., information related to the change rate or flow velocity of the circulation. Inter-frame differences are calculated and then superimposed on the original images in the form of a color display using a color table in which lower X-ray translucency (increased blood volume) is shown in warm colors, and negative changes, i.e., higher X-ray translucency (decreased blood volume) are shown in cool colors. As shown in Fig. 6, we can observe circulation-caused changes on the resulting velocity maps, showing a normal pattern of pulmonary and myocardial perfusion, which diffuses from the pulmonary arteries to the peripheral area.

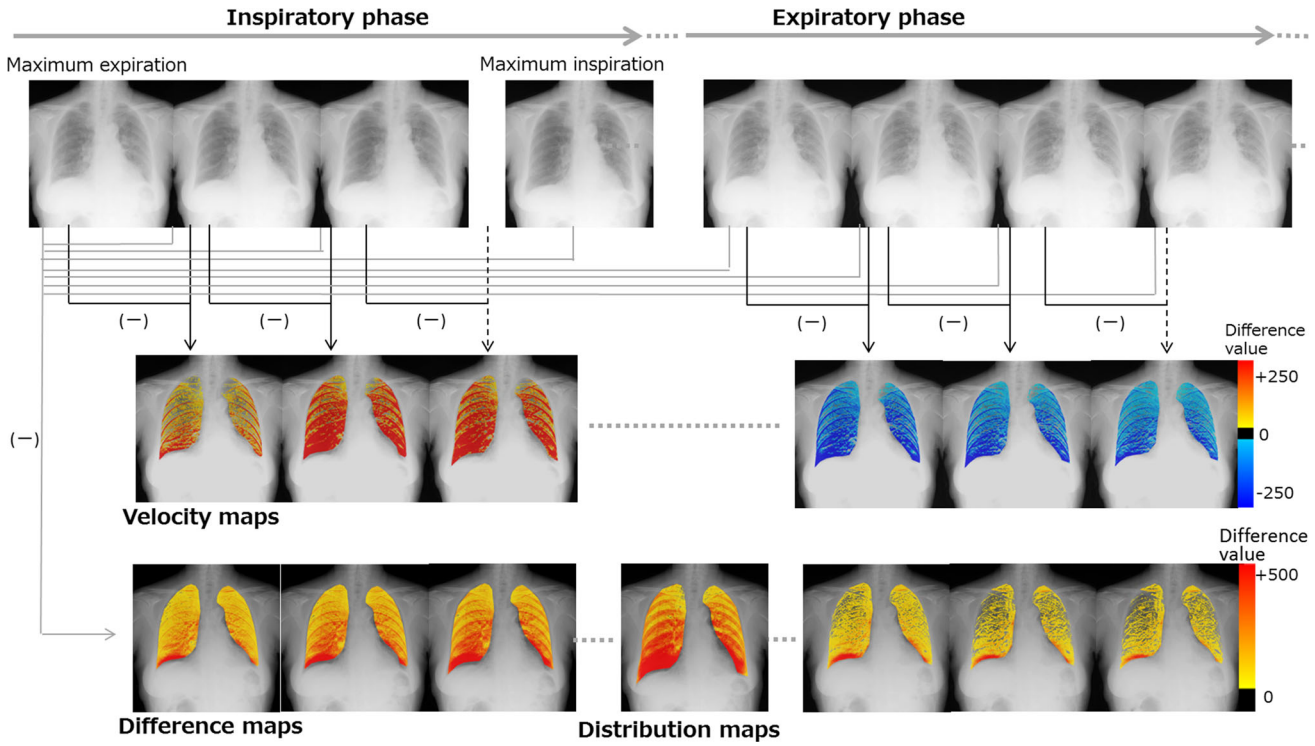

Fig. 5 Computer scheme for visualizing respiration-induced changes in pixel value

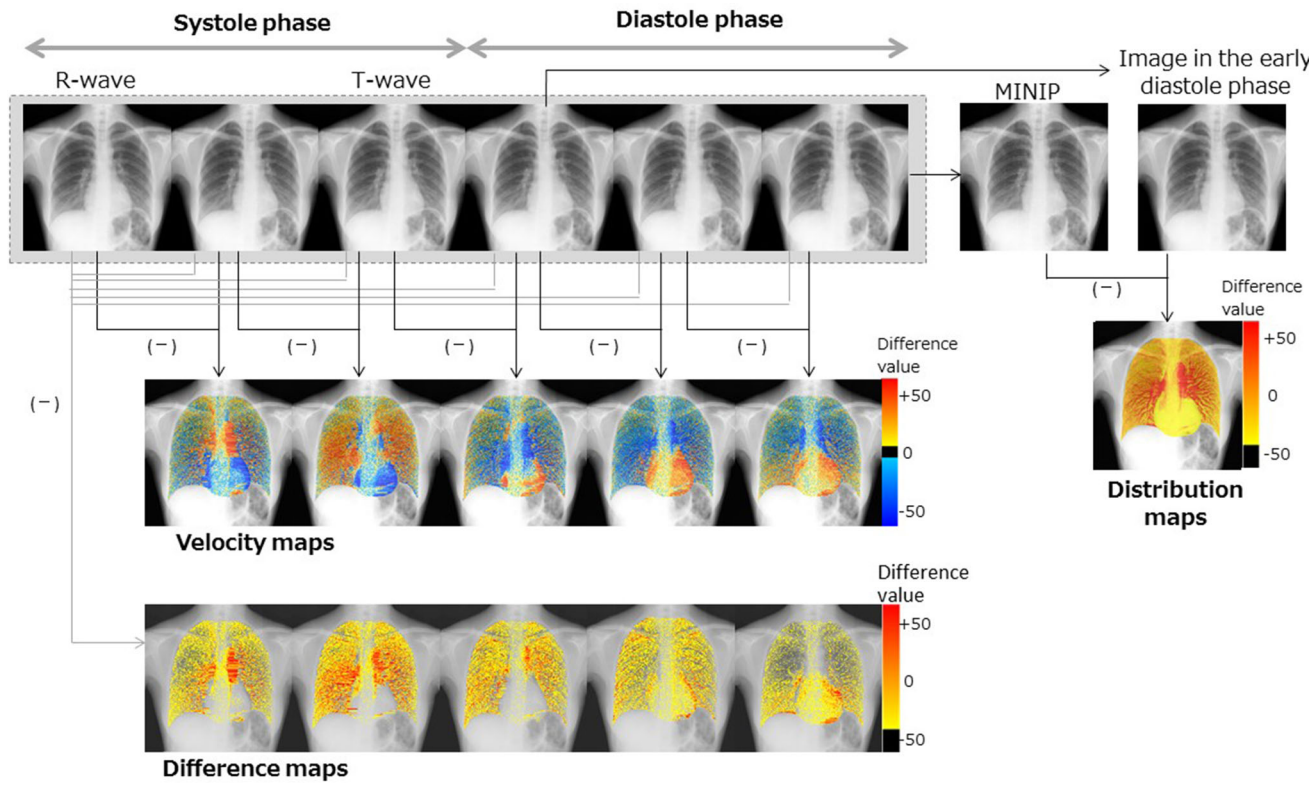

Fig. 6 Computer scheme for visualizing circulation -induced changes in pixel value (Japan patent JP4797173)

Image subtraction between two specific images creates another functional image, showing a distribution of circulation-caused changes in pixel value, i.e., information related to the perfusion distribution. For example, a minimum intensity projection (MinIP) image is created in one cardiac cycle, which composed of pixel values showing the least blood during one cardiac cycle. Thus, if image subtraction was performed between a MinIP image and an image at the early diastolic phase, the resulting distribution map would be created by the maximum differences in pixel value in the lungs during one cardiac cycle. We can also evaluate increases and decreases in circulation using image subtraction between sequential images with one specific image (e.g., an averaged image during one cardiac cycle, an image at the end of systolic or diastolic phases). A base image varies depending on the diagnostic purpose as well as analysis of the pulmonary ventilation. In any approach, distribution maps are also created by superimpose of the difference values on dynamic chest radiographs in the form of a color display.

4.2.3 Quantitative analysis

The above velocity and distribution maps are helpful for visual interpretation of the pulmonary function; however, they lack quantitation. One of the solutions is the use of analysis in block units, where pixel values are averaged in each block, tracking and deforming the ROI [25]. Figure 7 shows an example of block unit analysis. P (m, n) is the maximum difference in each block during a whole breathing or cardiac cycle. The percentage in differences of the pixel values to the summation of the results in all blocks is then calculated as

$$P_{\%}(m,n) = \frac{P(m,n)}{\sum_{n=0}^{N-1}\sum_{m=0}^{M-1} P(m,n)} \times 100 \quad (1)$$

where M and N are the numbers of blocks in the horizontal and vertical directions, respectively. In addition, m and n represent the coordinates of the blocks in the horizontal and vertical directions, respectively. Block unit analysis is useful for realizing a quantitative and statistical analysis as well as reducing the influence of movement, dilation, and contraction of vessels. In addition, it facilitates side-by-side and/or one-on-one comparison for computer-aided diagnosis (CAD) and V/Q study (described later). To facilitate visual evaluation, P (m, n) may be mapped on the original image in the same way as the velocity/distribution maps.

4.3 Detection of abnormalities

4.3.1 V/Q study

The ventilation-perfusion (V/Q) ratio is a very important diagnostic index for the evaluation of V/Q ratio, leading to the development of a treatment strategy in patients with pulmonary diseases. The V/Q ratio is usually calculated from the radioactivity count in lung scintigraphy. Functional imaging with a dynamic FPD has the potential for evaluating the V/Q ratio [29]. A V/Q map based changes in pixel value is provided by the use of resulting images of the ventilation and circulation distribution, i.e., as the ratio of ventilation to circulation distribution.

Figure 8 shows the results of pixel value-based V/Q study in a patient with a ventilation-perfusion mismatch (hypoxemia, 74-year-old man). In this case, the area of defective ventilation over the right lung was indicated as

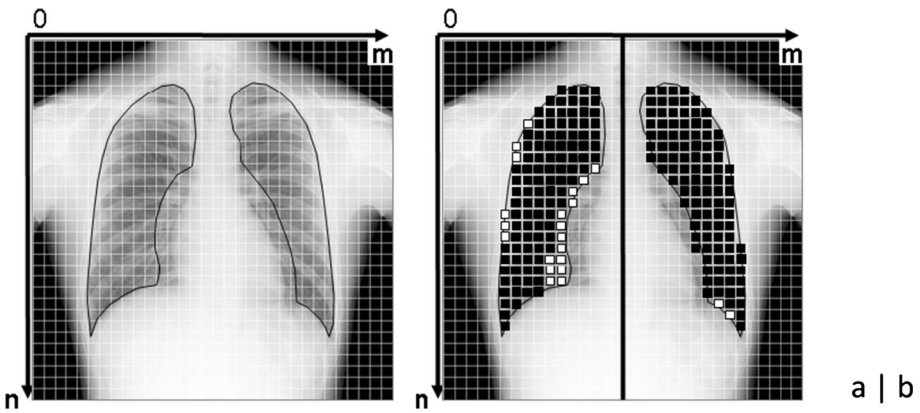

Fig. 7 One frame of dynamic chest radiographs divided into blocks that were slightly smaller than the intercostal space. (a) The black lines show the lung area determined for the measurement of pixel values in the lungs. The hilar regions are excluded from the lung area. (b) The bold vertical line shows the center of symmetry. "Symmetric positions" are pairs of blocks the same distance from the center of symmetry. The small black and white squares show the blocks with and without a pair for comparison, respectively

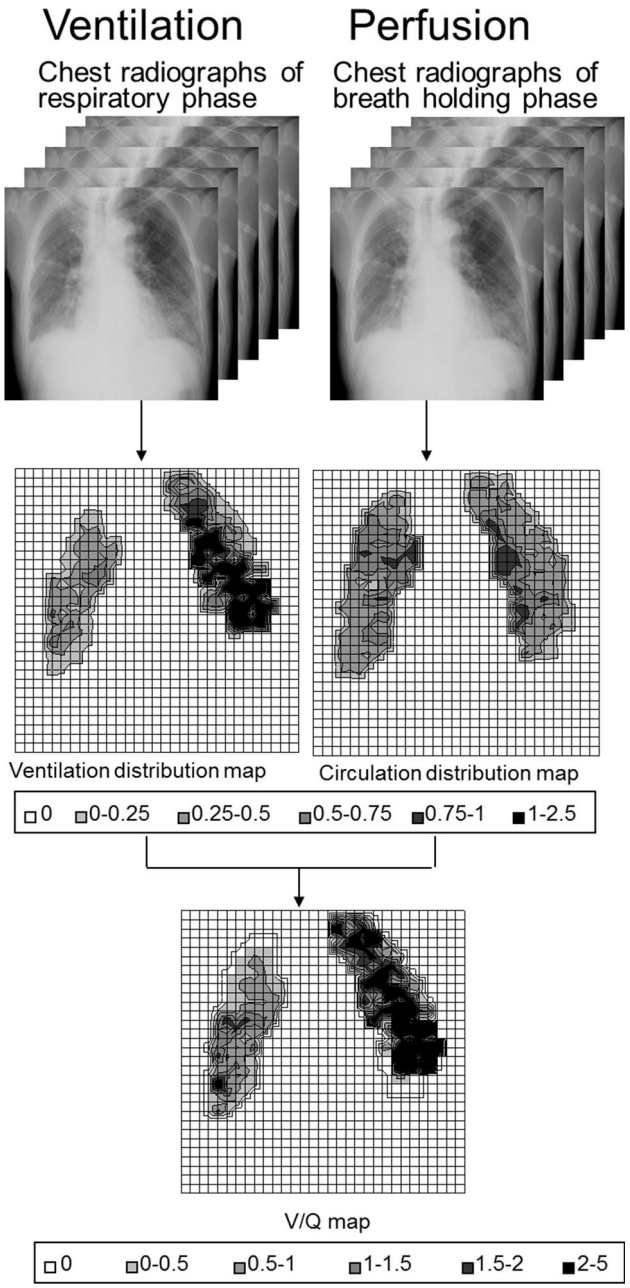

Fig. 8 The process of creating the V/Q map on the basis of changes in pixel value. V/Q map is created based on P %(m,n) calculated from Eq. 1

remarkably reduced changes in pixel value in the ventilation mapping image. In the result, the right lung showed lower V/Q ratio than that in the left lung. This finding indicates severe pulmonary impairment due to unbalanced V/Q, which was supported by the findings of the V/Q ratio calculated from lung scintigraphy [29].

4.3.2 Computer-aided diagnosis (CAD)

An accurate interpretation of dynamic chest radiographs requires a great deal of knowledge regarding respiratory and cardiac physiology. Thus, there is a great concern about the development of a CAD system for dynamic chest radiography. This development has just started, and only two trials have been reported. Tsuchiya et al. [59] developed a CAD system to detect lung nodules using dynamic chest radiographs taken during respiration. Their technique could quantitatively evaluate the kinetic range of nodules and was effective in detecting a nodule on dynamic images.

Another CAD system was to detect functional impairments in the ventilation and blood circulation in the lungs [25]. The results showed that unilateral abnormalities could be detected as a deviation from the right and left symmetry of respiration-induced changes in pixel value. However, for detecting bilateral abnormalities, further studies are required for the development of a multilevel detection method combined with several methods of pattern analysis.

5 Case report

Preliminary clinical trials have demonstrated that pulmonary impairment is successfully detected as decreased changes in pixel value in patients with pulmonary diseases, such as emphysema, asthma, and lung fibrosis [22–25], and that quantified diaphragm kinetics is also useful for the assessment of pulmonary function in patients with lung lobectomy. In this section, the results in a patient with pulmonary disease will be described in comparison with the typical findings found in normal controls.

Normally, ventilation color mapping images show a left-right symmetric distribution, with the color intensity increasing from the lung apex to the base of the lung, as shown in Fig. 5. The findings are reflection of normal pulmonary ventilation, which is greatest near the bottom of the lung and becomes progressively smaller toward the top with a symmetric right-and-left distribution [34, 35]. Circulation color mapping images also show a left-right symmetric distribution, with the color intensity decreasing from the pulmonary arteries to the peripheral area [60], reflecting normal perfusion, as shown in Fig. 6. In contrast, abnormal cases show nonuniform/asymmetric color distributions, which are different from the normal pattern. Figures 9, 10, 11 show the results in a patient with pleural adhesions in the left lung, resulting in a middle restricted ventilatory abnormality (74-year-old man). There are several findings of pleural adhesions in CT images (Fig. 12b, e–g). Lung scintigraphy shows marked reduction of ventilation as well as a reduced circulation in the right lung in comparison with the left lung (Fig. 12c). The right lung shows reduced changes in pixel value as well as a reduced intensity in the ventilation color mapping images (Fig. 9). The differences in respiratory changes in pixel value between the right and left lungs are also confirmed by ROI

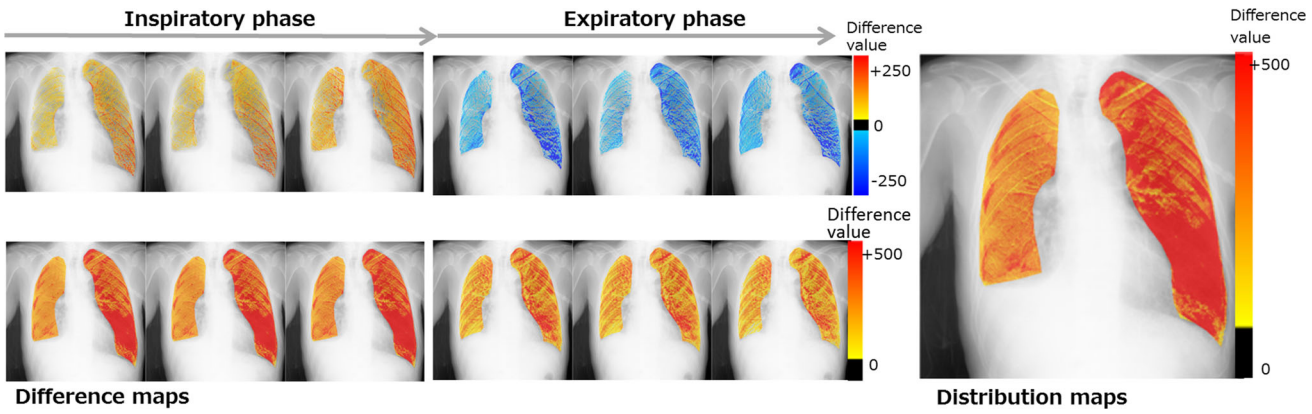

Fig. 9 Results of analysis of pulmonary ventilation

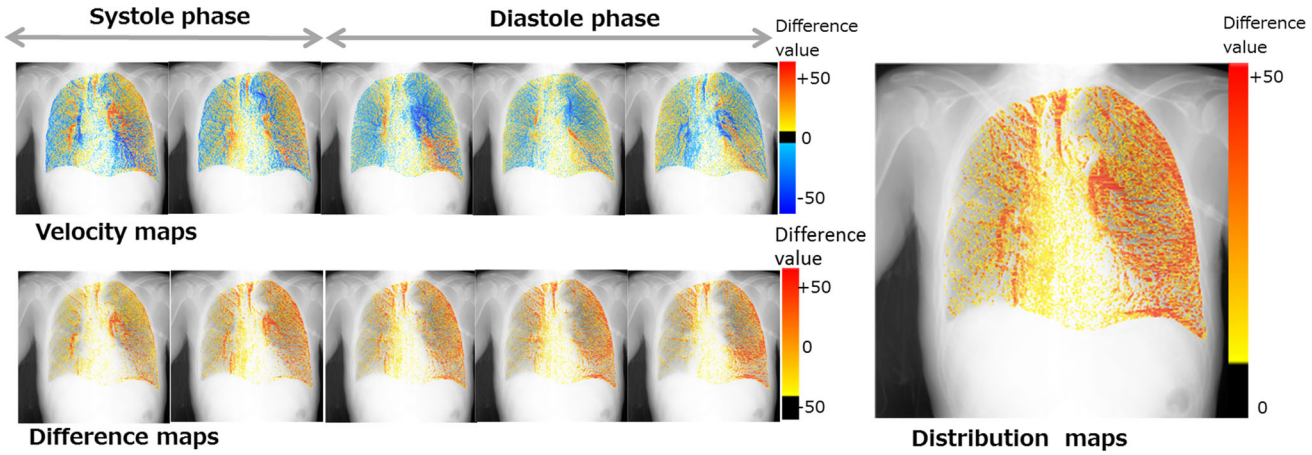

Fig. 10 Results of analysis of pulmonary circulation

Fig. 11 Measurement of averaged pixel value in ROIs located in the right and left lungs. The white squares indicate ROIs for the measurement

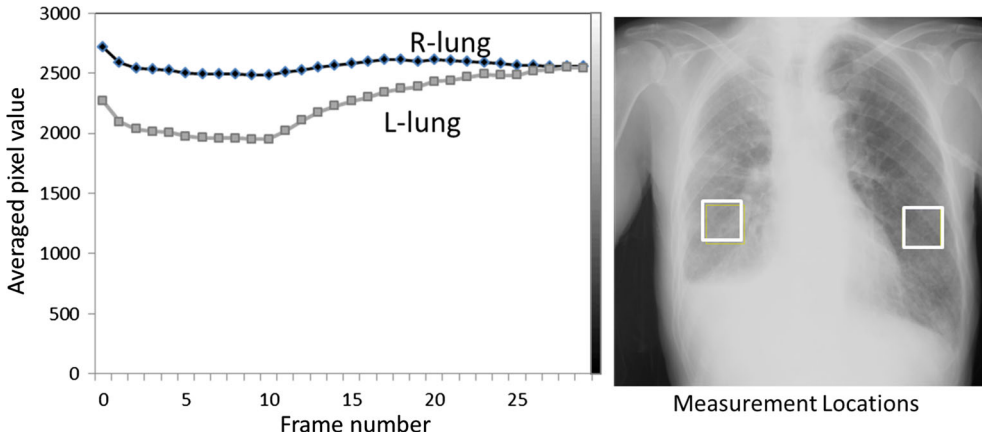

measurement, which is similar to lung densitometry as proposed by Siverman et al. [7–9] (Fig. 11). Furthermore, this patient had a reduced blood flow area in the right whole lung, as shown in Fig. 12d. The area appeared as a decrease in intensity in color mapping images during the breath-holding phase (Fig. 10).

6 Future potential of dynamic chest radiography

It is likely that dynamic chest radiography will be performed as an additional examination in the chest radiography. To meet a high demand for a portable use in clinical practice, particularly in emergency medicine, a

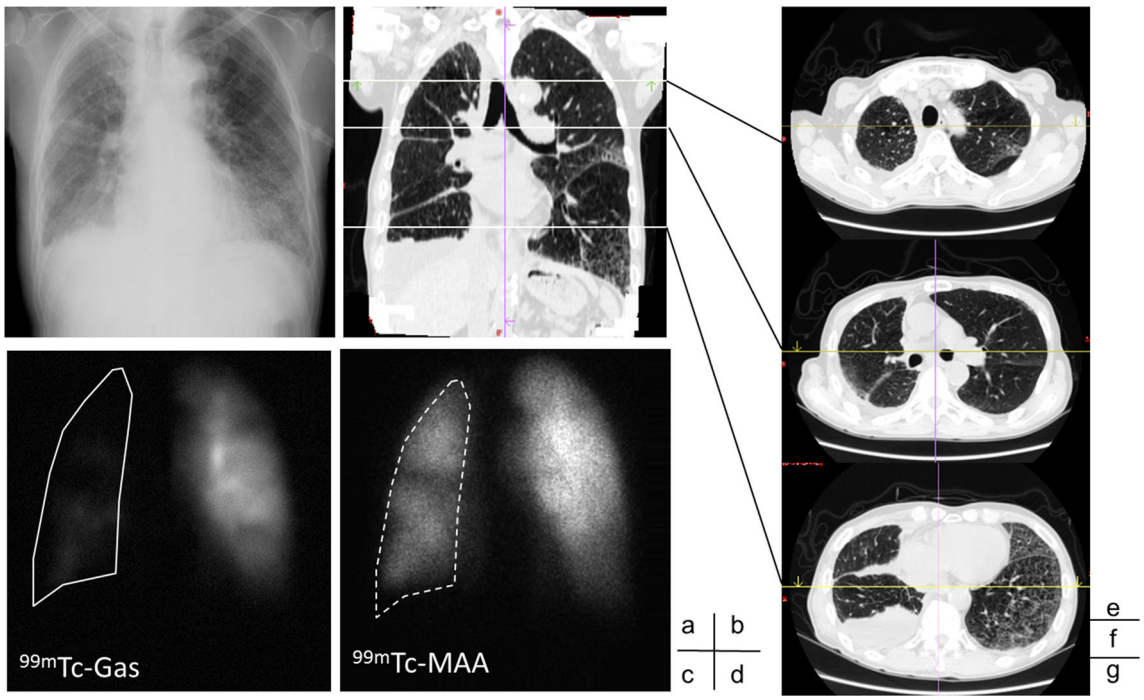

Fig. 12 Image findings of the patient with pleural adhesions (74-year-old man). (a) Chest radiograph, (b) CT image (coronal view), (c)-(d) ventilation and perfusion scintigrams. The right lung shows marked reduced ventilation (solid line) as well as reduced circulation (broken line). (e)-(g) CT images (axial views). There are several findings of pleural adhesions

portable dynamic chest radiography system will emerge in the near future. Dynamic chest radiography is certainly not the perfect functional imaging; lack of 3D information, no referring actual gas exchange nor perfusion (only relative functional information). These issues may be solved by the use of contrast media and advanced technologies, such as tomosynthesis and cone-beam CT. However, for dynamic chest radiography to be widely used in clinical situations, it is important to use simple procedures as much as possible so that clinicians have ready access to functional information just as if they used a stethoscope to assess pulmonary and/or cardiac abnormalities.

Radiologists and thoracic physicians may utilize dynamic chest radiography in two different ways. One is as a screening tool in health checkups. Patients are examined not only for detection of anatomic abnormalities, but also for the assessment of cardiopulmonary function. The total patient dose is about double that of conventional chest radiography; however, this is acceptable because of the increased yield of information.

Another use is as a follow-up tool for patients with pulmonary diseases. Dynamic chest radiography allows radiologists and thoracic physicians to evaluate the treatment effects and perioperative changes. One of the most important advantages of this functional imaging is that the imaging is performed in a manner similar to conventional chest radiography. Low-cost, small space and high-throughput functional X-ray imaging would lead to a reduction of medical costs, which is a potential advantage of dynamic chest radiography.

With dynamic chest radiography, image interpretation has transited from conventional estimation based on anatomic findings to evaluation based on dynamic changes. In this situation, computerized methods for quantifying cardiopulmonary function are essential for the implementation of dynamic chest radiography.

Some basic computer schemes have been demonstrated in this review paper. Specifically, image subtraction and color mapping techniques are useful for quantifying and visualizing slight changes in pixel value caused by respiration and circulation.

For further assistance to radiologists, it is urgent to develop CAD schemes designed for dynamic chest radiography. Another concern is an adverse effect of rib shadows. The presence of the ribs overlying or underlying soft tissues affects the quantitative analysis of pixel value in the lungs. In addition, the rib shadow prevents accurate inter-frame registration targeted for soft tissues because they move in a different manner during respiration. One of the solutions is the utilization of an advanced form of image processing for bone suppression, providing images that appear similar to dual-energy soft tissue images [61, 62]. Improved accuracy of motion tracking, texture analysis, and

analysis of rib kinematics has been confirmed in dynamic imaging combined with the bone suppression technique [63–65]. The computation time should be short for real-time processing by utilizing images preceding and following a present image.

Although the diagnostic performance of dynamic chest radiography has been addressed, the number of patients for whom it has been applied to so far is insufficient for the development of diagnostic criteria. Furthermore, it is likely that there is still a large amount of unused information that could be of real importance to clinicians and researchers. Dynamic chest radiography has been available technically and will be widely available in the near future. Further clinical studies are required which address the potential of dynamic chest radiography, along with the establishment of diagnostic logic. Successful application of dynamic chest radiography requires close collaboration of investigators familiar with technical matters and those familiar with anatomy, physiology, and clinical practice, for which this technique is being attempted to be applied.

There is an important issue related to the use of dynamic chest radiography both in clinical and research situations. The present method does not directly measure the gas exchanges in lung alveoli, or the actual perfusion; rather, it provides relative functional information related to pulmonary ventilation and circulation. Therefore, dynamic chest radiography should be used for the evaluation of intra-individual changes (e.g., follow-up examinations and/or side-by-side comparisons) rather than inter-individual differences, knowing the system capability as well as basic respiratory/circulation physiology.

Furthermore, it is not surprising if there are some differences between findings in dynamic chest radiography and those in lung scintigraphy. This is because the two are totally different in their imaging target, imaging mechanism, and imaging posture. In fact, such a difference has been reported in some clinical cases [24, 27]. The fact would rather be a great motivator for exploring respiratory and circulation physiology projected on dynamic chest radiographs. There are still many questions regarding the diagnostic performance of dynamic chest radiography which merit further research.

7 Conclusion

Dynamic chest radiography is a FPD based functional X-ray imaging, performed as an additional examination in chest radiography. Some of the most important advantages are: (1) imaging is performed in a manner similar to conventional chest radiography, (2) the total patient dose can be less than double the conventional one, and (3) pulmonary function can be assessed even without the use of contrast media. It is likely that there is still a large amount of unused information on dynamic chest radiographs during respiration. For utilizing it as a powerful and pertinent radiologic tool, further clinical studies are required which address the potential of dynamic chest radiography in collaboration with clinicians, physicists, and engineers.

Acknowledgments The author is grateful to the staff in the department of Radiology, Respiratory Medicine, and Respiratory Surgery, Clinical Laboratory, Kanazawa University Hospital, and staff from Canon Inc., for their assistance with clinical data acquisitions, and to Shigeru Sanada, PhD, for his frequent support over the course of the project, and Nobuo Okazaki, MD, for his intellectual debate on respiratory physiology. This work was supported in part by The Ministry of Education, Culture, Sports, Science and Technology, MEXT KAKENHI Grant Number 16K10271, 24601007, 19790860; JSPS Grant-in-Aid for Scientific Research on Innovative Areas (Multidisciplinary Computational Anatomy) JSPS KAKENHI Grant Number 15H01113; The Tateisi Science and Technology Foundation, Nakashima Foundation, Konica Minolta Science and Technology Foundation, Suzuken Memorial Foundation, Japan Cardiovascular Research Foundation, Nakatani Foundation, The Mitani Foundation for Research and Development, and The Mitsubishi Foundation.

Compliance with ethical standards

Conflict of interest The authors declare that they have no conflict of interest.

References

1. Kourilsky R, Marchalm M, Marchal MT. A new method of functional x-ray exploration of the lungs: photoelectric statidensigraphy. Dis chest. 1962;42:345–58.
2. Andrews AH, Jensik R, Pfisterer WH. Fluoroscopic pulmonary densiography. Dis chest. 1959;35:117–26.
3. Steiner RE, Laws JW, Gilbert J, Mcdonnell MJ. Radiologic lung-function studies. Lancet. 1960;2:1051–5.
4. Oderr C. Air trapping, pulmonary insufficiency and fluorodensimetry. Am J Roentgen. 1964;92:501–12.
5. George RB, Weill H, Tahir AH. Fluorodensimetric evaluation of regional ventilation in chronic obstructive pulmonary disease. South Med J. 1971;64:1161–5.
6. George RB, Weill H. Fluorodensimetry. A method for analyzing regional ventilation and diaphragm function. JAMA. 1971;217:171–6.
7. Silverman NR. Clinical video-densitometry pulmonary ventilation analysis. Radiology. 1972;103:263–5.
8. Silverman NR, Intaglietta M, Simon AL, Tompkins WR. Determination of pulmonary pulsatile perfusion by fluoroscopic videodensitometry. J Appl Physiol. 1972;33:147–9.
9. Silverman NR, Intaglietta M, Tompkins WR. Pulmonary ventilation and perfusion during graded pulmonary arterial occlusion. J Appl Physiol. 1973;34:726–31.
10. Rogers RM, Kuhl DE, Hyde RW, et al. Measurement of the vital capacity and perfusion of each lung by fluoroscopy and macroaggregated albumin lung scanning. An alternative to bronchospirometry for evaluating. Ann Intern Med. 1967;67:947–56.
11. Toffolo RR, Beerel FR. The autofluoroscope and 133-Xe in dynamic studies of pulmonary perfusion and ventilation. Radiology. 1970;94:692–6.

12. Lam KL, Chan HP, MacMahon H, et al. Dynamic digital subtraction evaluation of regional pulmonary ventilation with non-radioactive xenon. Invest. Radiolo. 1990;25:728–35.
13. Fujita H, Doi K, MacMahon H. Basic imaging properties of a large image intensifier-TV digital chest radiographic system. Invest. Radiol. 1987;22:328–35.
14. Bursch JH. Densitometric studies in digital subtraction angiography: assessment of pulmonary and myocardial perfusion. Herz. 1985;10:208–14.
15. Liang J, Jarvi T, Kiuru A, Kormano M, Svedström E. Dynamic chest image analysis: model-based perfusion analysis in dynamic pulmonary imaging. J Appl Signal Process. 1985;5:437–48.
16. Hoffmann KR, Doi K, Fencil LE. Determination of instantaneous and average blood flow rates from digital angiograms of vessel phantoms using distance-density curves. Invest Radiol. 1991;26:207–12.
17. Desprechins B, Luypaert R, Delree M, et al. Evaluation of time interval difference digital subtraction fluoroscopy patients with cystic fibrosis. Scand J Gastroenterol Suppl. 1988;143:86–92.
18. Kiuru A, Svedstrom E, Kuuluvainen I. Dynamic imaging of pulmonary ventilation. Description of a novel digital fluoroscopic system. Acta Radiol. 1991;32:114–9.
19. Kiuru A, Svedstrom E, Korvenranta H, et al. Dynamic pulmonary imaging: performance properties of a digital fluoroscopy system. Med Phys. 1992;19:467–73.
20. Vano E, Geiger B, Schreiner A, et al. Dynamic flat panel detector versus image intensifier in cardiac imaging: dose and image quality. Phys Med Biol. 2005;50:5731–42.
21. Srinivas Y, Wilson DL. Image quality evaluation of flat panel and image intensifier digital magnification in x-ray fluoroscopy. Med Phys. 2002;29:1611–21.
22. Tanaka R, Sanada S, Okazaki N, Kobayashi T, Fujimura M, Yasui M, Matsui T, Nakayama K, Nanbu Y, Matsui O. Evaluation of pulmonary function using breathing chest radiography with a dynamic flat-panel detector (FPD): primary results in pulmonary diseases. Invest Radiol. 2006;41:735–45.
23. Tanaka R, Sanada S, Okazaki N, Kobayashi T, Nakayama K, Matsui T, Hayashi N, Matsui O. Quantification and visualization of relative local ventilation on dynamic chest radiographs. In: The international society for optical engineering. Medical imaging. Proceedings of SPIE. Vol. 6143, No. 2; 2006. p. 1–8 (**62432Y**).
24. Tanaka R, Sanada S, Fujimura M, Yasui M, Nakayama K, Matsui T, Hayashi N, Matsui O. Development of functional chest imaging with a dynamic flat-panel detector (FPD). Radiol Phys Technol. 2008;1:137–43.
25. Tanaka R, Sanada S, Fujimura M, Yasui M, Tsuji S, Hayashi N, Okamoto H, Nanbu Y, Matsui O. Ventilatory impairment detection based on distribution of respiratory-induced changes in pixel values in dynamic chest radiography: a feasibility study. IJCARS. 2011;6:103–10.
26. Tanaka R, Sanada S, Tsujioka K, Matsui T, Takata T, Matsui O. Development of a cardiac evaluation method using a dynamic flat-panel detector (FPD) system: a feasibility study using a cardiac motion phantom. Radiol Phys Technol. 2008;1:27–32.
27. Tanaka R, Sanada S, Fujimura M, Yasui M, Tsuji S, Hayashi N, Okamoto H, Nanbu Y, Matsui O. Pulmonary blood flow evaluation using a dynamic flat-panel detector: feasibility study with pulmonary diseases. IJCARS. 2009;4:449–54.
28. Tanaka R, Sanada S, Fujimura M, Yasui M, Tsuji S, Hayashi N, Okamoto H, Nanbu Y, Matsui O. Development of pulmonary blood flow evaluation method with a dynamic flat-panel detector (FPD): quantitative correlation analysis with findings on perfusion scan. Radiol Phys Technol. 2010;3:40–5.
29. Tanaka R, Sanada S, Fujimura M, Yasui M, Tsuji S, Hayashi N, Okamoto H, Nanbu Y, Matsui O. Ventilation-perfusion study without contrast media in dynamic chest radiography. In: The international society for optical engineering. Medical imaging. Proceedings of SPIE. Vol. 7965; 2011. p. 1–7 (**79651Y**).
30. Tanaka R., Sanada S, Kobayashi T, Suzuki M, Matsui T, Hayashi N, Nanbu Y. Automated analysis for the respiratory kinetics with the screening dynamic chest radiography using a flat-panel detector system. In: Computer Assisted Radiology and Surgery. Proceeding; 2003. 179–186.
31. Tanaka R, Sanada S, Kobayashi T, Suzuki M, Matsui T, Inoue H. Breathing chest radiography using a dynamic flat-panel detector (FPD) with computer analysis for a screening examination. Med Phys. 2004;31:2254–62.
32. Tanaka R, Sanada S, Kobayashi T, Suzuki M, Matsui T, Matsui O. Computerized methods for determining respiratory phase on dynamic chest radiographs obtained by a dynamic flat-panel detector (FPD) system. J Digit Imaging. 2006;19:41–51.
33. Fraser RS, Muller NL, Colman NC, Pare PD. Fraser and Pare's Diagnosis of Diseases of the Chest. 4th ed. W.B. Saunders Company: Philadelphia, London, New York, St. Louise, Sydney, and Toronto; 1999.
34. West JB. Ventilation—how gas gets to the alveoli. Respiratory physiology: the essentials. 3rd ed. Philadelphia: Lippincott Williams & Wilkinss; 2000. p. 11–9.
35. Squire LF, Novelline RA. Fundamentals of Radiology, 4th ed. Harvard University: Cambridge, Massachusetts, and London; 1988.
36. Hansen JT, Koeppen BM. Cardiovascular Physiology, In: Netter's Atlas of Human Physiology (Netter Basic Science). Icon Learning Systems: Teterboro, New Jersey; 2002.
37. Tanaka R, Sanada S, Okazaki N, Kobayashi T, Suzuki M, Matsui T, Matsui O. Detectability of regional lung ventilation with flat-panel detector-based dynamic radiography. J. Digit. Imag. 2008;21:109–20.
38. Heyneman LE. The chest radiograph: Reflections on cardiac physiology. In: Radiological Society of North America. Scientific Assembly and Annual Meeting Program; 2005, p. 145.
39. Goodman LR. Felson's principles of chest roentgenology, a programmed text. London, Toronto, Philadelphia: W B Saunders Co; 2006.
40. Turner AF, Lau FY, Jacobson G. A method for the estimation of pulmonary venous and arterial pressures from the routine chest roentgenogram. Am J Roentgenol Radium Ther Nucl Med. 1972;116:97–106.
41. Chang CH. The normal roentgenographic measurement of the right descending pulmonary artery in 1085 cases. Am J Roentgenol Radium Ther Nucl Med. 1962;87:929–35.
42. Pistolesi M, Milne EN, Miniati M, Giuntini C. The vascular pedicle of the heart and the vena azygos. Part II: Acquired heart disease. Radiology. 1984;152:9–17.
43. Kawashima H, Tanaka R, Matsubara K, et al. Temporal-spatial characteristic evaluation in a dynamic flat-panel detector system. In: The international society for optical engineering. Medical imaging. Proceedings of SPIE. Vol. 7622; 2010. p. 1–8 (**76224T**).
44. International basic safety standards for protection against ionizing radiation and for the safety of radiation sources. International atomic energy agency (IAEA): Vienna; 1996.
45. Xu XW, Doi K. Image feature analysis for computer-aided diagnosis: accurate determination of ribcage boundary in chest radiographs. Med Phys. 1995;22:617–26.
46. Li L, Zheng Y, Kallergi M, Clark RA. Improved method for automatic identification of lung regions on chest radiographs. Acad Radiol. 2001;8:629–38.
47. Katsuragawa S, Doi K, MacMahon H. Image feature analysis and computer-aided diagnosis in digital radiography: detection and characterization of interstitial lung disease in digital chest radiographs. Med Phys. 1988;15:311–9.
48. Katsuragawa S, Doi K, MacMahon H. Image feature analysis and computer-aided diagnosis in digital radiography: classification of

normal and abnormal lungs with interstitial disease in chest images. Med Phys. 1989;16:38–44.
49. Katsuragawa S, Doi K, Nakamori N, MacMahon H. Image feature analysis and computer-aided diagnosis in digital radiography: effect of digital parameters on the accuracy of computerized analysis of interstitial disease in digital chest radiographs. Med Phys. 1990;17:72–8.
50. Ashizawa K, Ishida T, MacMahon H, Vyborny CJ, Katsuragawa S, Doi K. Artificial neural networks in chest radiology: application to the differential diagnosis of interstitial lung disease. Acad Radiol. 1999;6:2–9.
51. Ishida T, Katsuragawa S, Kobayashi T, MacMahon H, Doi K. Computerized analysis of interstitial disease in chest radiographs: improvement of geometric-pattern feature analysis. Med Phys. 1997;24:915–92.
52. Nakamori N, Doi K, MacMahon H, Sasaki Y, Montner S. Effect of heart size parameters computed from digital chest radiographs on detection of cardiomegaly: potential usefulness for computer–aided diagnosis. Invest Radiol. 1991;26:546–50.
53. Kano A, Doi K, MacMahon H, Hassell DD, Giger ML. Digital image subtraction of temporally sequential chest images for detection of interval change. Med Phys. 1994;21:453–61.
54. Ishida T, Ashizawa K, Engelmann R, Katsuragawa S, MacMahon H, Doi K. Application of temporal subtraction for detection of interval changes on chest radiographs: improvement of subtraction images using automated initial image matching. J Digit Imaging. 1999;12:77–86.
55. Rank K, Unbehauen R. An adaptive recursive 2-D filter for removal of Gaussian noise in images. IEEE Trans Image Process. 1992;1:431–6.
56. Hoffmann KR, Doi K, Chen SH, Chan HP. Automated tracking and computer reproduction of vessels in DSA images. Invest Radiol. 1990;25:1069–75.
57. Chen QS, Weinhous MS, Deibel FC, Ciezki JP, Macklis RM. Fluoroscopic study of tumor motion due to breathing: facilitating precise radiation therapy for lung cancer patients. Med Phys. 2001;28:1850–6.
58. Richter A, Wilbert J, Baier K, et al. Feasibility study for markerless tracking of lung tumors in stereotactic body radiotherapy. Int J Radiat Oncol Biol Phys. 2010;78:618–27.
59. Tsuchiya Y, Kodera Y, Tanaka R, Sanada S. Quantitative kinetic analysis of lung nodules using the temporal subtraction technique in dynamic chest radiographies performed with a flat panel detector. J. Digit. Imag. 2009;2:126–35.
60. Tanaka R, Sanada S, Oda M, Suzuki M, Sakuta K, Kawashima H, Iida H. “Circulation map” projected on functional chest radiography with a dynamic FPD. ECR Electron Poster Present. 2013;. doi:10.1594/ecr2013/C-0279.
61. Suzuki K, Abe H, MacMahon H, Doi K. Image-processing technique for suppressing ribs in chest radiographs by means of massive training artificial neural network (MTANN). IEEE Trans Med Imaging. 2006;25:406–16.
62. Knapp J, et.al. Feature Based Neural Network Regression for Feature Suppression, U.S. Patent Number, 8,204,292 B2; 2012.
63. Tanaka R, Sanada S, Sakuta K, Kawashima H. Improved accuracy of markerless motion tracking on bone suppression images: preliminary study for image-guided radiation therapy (IGRT). Phys Med Biol. 2015;60:N209–18.
64. Tanaka R, Sanada S, Sakuta K, Kawashima H, Kishitani Y. Low-dose dynamic chest radiography combined with bone suppression technique. ECR Electron Poster Present. 2015;. doi:10.1594/ecr2015/C-0239.
65. Tanaka R, Sanada S, Sakuta K, Kawashima H. Quantitative analysis of rib kinematics based on dynamic chest bone images: preliminary results. J Med Imaging. 2015;2:024002.